Optoelectronic properties of C 66 H 54 Br 6 N 6 O 12 supramolecular nanotube by DFT studies

H. A. Rahnamaye Aliabad (✉ Rahnama@hsu.ac.ir)

Hakim Sabzevari University

H. Vahidi

Hakim Sabzevari University

Abstract

In this work, the structural and optoelectronic properties of $C_{66}H_{54}Br_6N_6O_{12}$ nanotubes, which is in the triclinic phase, have been studied by the Perdew- Burke- Ernzrhof Generalized Gradient Approximation (PBE- GGA). The semi metallic behaviors and the flat bands are observed in the band structure with 2.06 eV band gap. From the optical spectra, this nanotube is birefringence with Plasmon energies of 23.41, 23.36 and 23.55 eV at x, y and z direction, respectively. Cauchy coefficients have been obtained in the wavelength range of 550 to 850 nm. The results show that this nanotube cab be used in the optoelectronic devices like metallic carbon nanotube and glasses.

1. Introduction

Nanotubes are a group of nanomaterials composed of graphene rolls that were first observed in 1991 by Iijima [1]. This particular type of material is generally divided into two categories, single walled nanotube (SWNT) and multi walled nanotube (MWNT), each with its own characteristics [2−4].

Nanotube-based nanostructures have features such as high hardness, electrical conductivity, and thermal conductivity [5]. One of the ways to obtain a Supramolecular nanotube from the halo-hydrocarbon assembly is to rotate one unit at a specific angle and to position it in a column [6, 7]. This is how the $C_{66}H_{54}Br_6N_6O_{12}$ compound is made. Because of clean energy is becoming a necessity in today's world, thermoelectric materials such as nanotubes with high-emission merit ZT can be used to convert heat into electrical energy [8, 9]. This class of materials has structural, optical and thermoelectrical properties such as drug delivery, optical memory, solar cells, gas storage and… [10−14]. Yuan Sun et al, study about assembly of Camptothecin (natural quinoline alkaloid with potent anti-tumor activity that functions through the inhibition of DNA topoisomerase) by nanotubes produced human serum that shown high potential against several human cancer cell types [15]. Lukang Ji et al demonstrate a cooperative energy and chirality transfer by constructing a supramolecular light-harvesting chiral nanotube in the aqueous phase. They assembled two achiral acceptors that have different energy bands with the nanotube that led to transfer its chirality to both of the acceptors [16−19].

In this work, the electronical and optical properties of $C_{66}H_{54}Br_6N_6O_{12}$ nanotube including band structure, density of states, dielectric function, refractive index, extinction coefficient and eloss have been studied by Wien2k package [15]. One method for optimization of the optoelectronic properties of compounds is figure out them with energy and wavelength on lattice structure. One of the main aims of this work is investigation of optoelectronic properties by energy.

2. Method Of Calculations

Calculations of this work were executed by full potential linearized augmented plane wave (FP-LAPW) method in the framework of density functional theory for the structural, electronic and thermoelectric properties of $C_{66}H_{54}Br_6N_6O_{12}$ compound with Wien2k package [20]. Exchange-correlation potential is a

challenge to solve the Schrödinger equation. We used the generalized gradient approximation (GGA) to resolve this ambiguity to have an accurate band gap [21, 22]. The cut-off energy for separation of the valence and core states, has chosen − 6 Ry. For calculation of electronic properties, 400 k-points is used in the first Brillouin zone and $R_{MT×} K_{max}$ = 7 where R_{MT} is the smallest muffin-tin radius and K_{max} is the cut-off for the plane wave. The muffin-tin radii for C, H, Br, N and O were 1.02, 0.06, 1.60, 1.31 and 1.13 a.u., respectively. Crystal structure of $C_{66}H_{54}Br_6N_6O_{12}$ were shown in Fig. 1.

Optical properties of materials such as refractive index and energy dissipation spectrum can be obtained by dielectric tensor that has been obtained from the transition between the occupied and unoccupied states in the energy band [23]. The imaginary and real parts of the dielectric function defined as:

$$\epsilon_{12}\left(\omega\right) = \epsilon_1\left(\omega\right) + i\epsilon_2\left(\omega\right)$$

1

$$\epsilon_1\left(\omega\right) = \sigma_{ij} + \frac{2}{\pi}P\int_0^\infty \frac{\omega'\epsilon_{ij}''\left(\omega\right)}{\omega'^2 - \omega^2}d\omega'$$

2

$$\epsilon_2\left(\omega\right) = \frac{4\pi e^2}{m^2\omega^2}\sum_{c,v}\int dk < c_k\left|P^\alpha\right|v_k>< v_k\left|P^\alpha\right|c_k > \delta(\epsilon_{c_k} - \epsilon_{v_k} - \omega)$$

3

In the above relations P represents the Cauchy integral part and σ is the optical conductivity. $|c_k>$ and $|v_k>$ are electron states in the capacitance band and the conduction band, respectively.

By imaginary and real parts of the dielectric function we can find refractive index and extinction coefficient:

$$n\left(\omega\right) = \frac{1}{\sqrt{2}}\left[\sqrt{\epsilon_1^2\left(\omega\right) + \epsilon_2^2\left(\omega\right)} + \epsilon_1\left(\omega\right)\right]^{\frac{1}{2}}$$

4

$$k\left(\omega\right) = \frac{1}{\sqrt{2}}\left[\sqrt{\epsilon_1^2\left(\omega\right) + \epsilon_2^2\left(\omega\right)} - \epsilon_1\left(\omega\right)\right]^{\frac{1}{2}}$$

5

Furthermore, ELF (L) can be Extracted using refractive index and extinction coefficient [24, 25] as below:

$$L = -Im \left(\frac{1}{\epsilon_1 + i\epsilon_2} \right) = \frac{\epsilon_2}{\epsilon_1^2 + \epsilon_2^2}$$

6

3. Structural And Electronic Results

The band structure of $C_{66}H_{54}Br_6N_6O_{12}$ compound is plotted along the symmetry lines shown in Fig. 2. The Fermi energy is selected as the origin and is located above the valence band. The band gap, which is the distance between top of valence band and the bottom of the conduction band, is below the Fermi level. As can be seen in Fig. 2, a band of energy is created in energy of 1.45 which is not observed in the density of states. If we consider this string of band as the top of the conduction band, the value of the band gap will be 1.45 eV; and by regardless of that, the size of the band gap will be 2.06 eV, which is in good agreement with the density of states. It should be noted that no experimental sample of this compound has been made so far. The nature of the band gap obtained is indirect along G-M.

The area under the density of states curve for each energy indicates the number of states permitted for the presence of the electron in that energy range. The DOS of the $C_{66}H_{54}Br_6N_6O_{12}$ from − 25 to 20 eV shown in Fig. 3 by GGA. The band gap calculated in DOS is 1.74 eV which is in good agreement with the band structure of the compound desired.

In Fig. 4, the calculated density of states (DOS) is displayed for the $C_{66}H_{54}Br_6N_6O_{12}$ compound for each atom. According to the obtained spectra, N- 2s and Br- 4s in -22.8 to -21.8 eV and − 20 to -19.8 eV energy range is composed the lowest valence states. The top of the valence bands is made up by the Br- 4p and H- 1s state and the top of the valence bands is made up by the Br- 4p state and the bottom of the conduction band is mainly composed of by the C- 2s state.

4. Optical Results

The dielectric function is used to describe the material's response to the electric field [26]. Because of $C_{66}H_{54}Br_6N_6O_{12}$ compound has a triclinic crystal structure so that lattice parameters are different from one another therefor dielectric functions along x, y and z direction are different. In the real part of the dielectric function, maximum and minimum values are about x direction which are in energies 3.08 and 17.26 eV, respectively. In the imaginary part of the dielectric function, the peaks represent the optical transitions allowed between occupied strips and empty modes which are in 3.33, 4.50 and 6.70 eV in x direction.

The refractive index of any material expresses the behavior of that material with respect to wave and electromagnetism. The refractive index is attributed to the environment where light refraction occurs at the boundary of the environment [27]. refractive index of $C_{66}H_{54}Br_6N_6O_{12}$ compound in terms of

wavelength were shown in 3 direction by Fig. 6. Cauchy's coefficients in all three directions are calculated for the refractive index by below formula:

$$n\left(\lambda\right) = A + \frac{B}{\lambda^2} + \frac{C}{\lambda^4}$$

7

A, B and C constants are known as Cauchy's coefficients [28].

Table 1
Cauchy's coefficients for refractive index

	λ (nm):550 to 750	λ (nm):550 to 850	λ (nm): 600 to 800
	x direction	y direction	z direction
A:	1.931	1.71	1.858
B:	-67778.341	18782.013	-109702.316
C:	31847634236.641	27264415795.807	51417106307.436

The extinction coefficient for a material is a measure of the amount of electromagnetic radiation absorbed by that material. If the electromagnetic beam passes easily through the material, the material has a low extinction coefficient. The diagram of this parameter is in the part a of Fig. 7.

The extinction coefficient of a substance is similar to the imaginary part of the dielectric function. The peaks of the extinction coefficient in Fig. 7 show the transitions between the band. Table 2 shows the energy of the peaks, which is in good agreement with the results of the imaginary part of the dielectric function.

Table 2
Peaks of energy for extinction coefficient

	Energy (eV)		
	x direction	y direction	z direction
First transition	3.36 eV	2.57 eV	2.78 eV
Second transition	4.74 eV	5.21 eV	5.21 eV
Third transition	6.97 eV	5.72 eV	5.91 eV
Fourth transition	16.28 eV	15.85 eV	14.76 eV

Electron energy loss spectrum *EELS* is an optical spectrum [29, 30] used to Getting Plasmon energy. It is a technique that determination the change in kinetic energy of electrons. The electron density is so

important to obtain the plasmon excitation.

In part b of Fig. 7, we calculated EEL spectra in x, y and z direction. Energy of main peak that represents plasmon peaks in x, y and z direction are 23.41, 23.36 and 23.55 eV, respectively. In this energy range, the real part of the dielectric function is close to zero.

The ratio of the radiant energy absorbed by an object to the total radiant energy that falls on the object is called the absorption coefficient. The absorption coefficient depends on the characteristics of the body surface. part a of Fig. 8 is showed Absorption coefficient of $C_{66}H_{54}Br_6N_6O_{12}$ compound in x, y and z directions. Due to the absorption of photons by matter, the electron moves from the capacitance band to the conduction band. The absorption of photons by the electron is called inter-band absorption. The adsorption process begins after the band gap range; Because the band gap in the restricted area is empty of energy levels. Absorption peaks in the $C_{66}H_{54}Br_6N_6O_{12}$ composition are around 17 eV. Maximum optical absorption of the desired composition in x, y and z directions are located in 16.45, 16.87 and 16.87 eV, respectively.

The reflection coefficient determines the amplitude of the wave or the intensity of the reflected wave relative to the radiation wave. part b of Fig. 8 is showed reflection coefficient of $C_{66}H_{54}Br_6N6O_{12}$ compound in x, y and z directions. The maximum of reflectivity is about x direction that is located in 17.26 eV. The behavior of this quantity is relatively similar in the y and z direction.

Conclusion

structural and optoelectronic properties of $C_{66}H_{54}Br_6N_6O_{12}$ compound, which is in the triclinic phase, is calculated by using density functional theory that generalized gradient approximation (GGA) is used to obtain the exchange correlation potential. The results of the band structure indicate that an indirect band gap is created at the bottom of the Fermi surface and its value is measured as 2.06 eV, while in the density of states, the value of 1.74 eV is measured for the band gap that is close to each other. In the real part of the dielectric function, maximum values are about x direction which is in energy 3.08 eV. the optical transitions that obtained from imaginary part of the dielectric function are in 3.33, 4.50 and 6.70 eV in x direction. Cauchy coefficients in the wavelength range of 550 to 850 nm have been obtained that correspond to the refractive index range in this region. Maximum optical absorption is located in 16.87 eV for both y and z axes.

Declarations

Acknowledgments

Ethics approval and consent to participate:

Not applicable

Consent for publication:

Not applicable

Availability of data and materials:

Not applicable

Competing interests:

The authors declare that they have no competing interests

Funding:

Not applicable

Code availability:

Wien2k software

Authors' contributions:

All authors read and approved the final manuscript. H. A. Rahnamaye Aliabad supervised the findings of this work and wrote the manuscript. H. Vahidi performed the computations by using Wien2k software.

References

1. Iijima, S.: Carbon nanotubes: past, present, and future. Phys. B: Condens. Matter. **323**(1), 1–5 (2002 Oct)
2. Chio, L., Pinals, R.L., Murali, A., Goh, N.S., Landry, M.P.: Covalent Surface Modification Effects on Single-Walled Carbon Nanotubes for Targeted Sensing and Optical Imaging. Adv. Funct. Mater. **30**(17), 1910556 (2020 Apr)
3. Liu, X., Mohammed, H.I., Ashkezari, A.Z., Shahsavar, A., Hussein, A.K., Rostami, S.: An experimental investigation on the rheological behavior of nanofluids made by suspending multi-walled carbon nanotubes in liquid paraffin.Journal of Molecular Liquids. 2020 Feb15;300:112269
4. Chae, H.G., Sreekumar, T.V., Uchida, T., Kumar, S.: A comparison of reinforcement efficiency of various types of carbon nanotubes in polyacrylonitrile fiber. Polymer. 2005 Nov 21;46(24):10925-35
5. Mihajlovic, M., Mihajlovic, M., Dankers, P.Y., Masereeuw, R., Sijbesma, R.P.: Carbon nanotube reinforced supramolecular hydrogels for bioapplications. Macromol. Biosci. **19**(1), 1800173 (2019 Jan)

6. Liu, Z., Liu, G., Wu, Y., Cao, D., Sun, J., Schneebeli, S.T., Nassar, M.S., Mirkin, C.A., Stoddart, J.F.: Assembly of supramolecular nanotubes from molecular triangles and 1, 2-dihalohydrocarbons. J. Am. Chem. Soc. **14**(47), 16651−16660 (2014 Nov)

7. Rodriguez-Vazquez, N., Lionel Ozores, H., Guerra, A., Gonzalez-Freire, E., Fuertes, A., Panciera, M., Priegue, M., Outeiral, J., Montenegro, J., Garcia-Fandino, J., Amorin, R.: M. Membrane-targeted self-assembling cyclic peptide nanotubes. Current topics in medicinal chemistry. Dec 1;14(23):2647-61. (2014)

8. Abareshi, A., Aliabad, H.R.: Anisotropic thermoelectric properties of Sr5Sn2As6 compound under pressure by PBE-GGA and mBJ approaches. Mater. Res. Express. **25**(9), 096303 (2017 Sep)

9. Culebras, M., Cho, C., Krecker, M., Smith, R., Song, Y., Gómez, C.M., Cantarero, A., Grunlan, J.C.: High thermoelectric power factor organic thin films through combination of nanotube multilayer assembly and electrochemical polymerization. ACS applied materials & interfaces. 2017 Feb 9;9(7):6306-13

10. Harito, C., Bavykin, D.V., Yuliarto, B., Dipojono, H.K., Walsh, F.C.: Polymer nanocomposites having a high filler content: synthesis, structures, properties, and applications. Nanoscale. **11**(11), 4653−4682 (2019)

11. Abdullah, L.A.: Nonlinear Optical Properties of Liquid Crystal doped with different concentrations of carbon nanotubes. InAIP Conference Proceedings 2019 Jul 17 (Vol. 2123, No. 1, p. 020064). AIP Publishing LLC

12. Bazli, L., Siavashi, M., Shiravi, A.: A Review of Carbon Nanotube/TiO2 Composite Prepared via Sol-Gel Method. J. Compos. Compd. **28**(1), 1−0 (2019 Oct)

13. Panda, T., Kundu, T., Banerjee, R.: Self-assembled one-dimensional functionalized metal−organic nanotubes (MONTs) for proton conduction. Chem. Commun. **48**(44), 5464−5466 (2012)

14. Zaworotko, M.J.: Materials science: designer pores made easy.Nature. 2008Jan;451(7177):410

15. Sun, Y., Shieh, A., Kim, S.H., King, S., Kim, A., Sun, H.L., Croce, C.M., Parquette, J.R.: The self-assembly of a camptothecin-lysine nanotube.Bioorganic & medicinal chemistry letters. 2016 Jun15;26(12):2834−8

16. Ji, L., Sang, Y., Ouyang, G., Yang, D., Duan, P., Jiang, Y., Liu, M.: Cooperative Chirality and Sequential Energy Transfer in a Supramolecular Light-Harvesting Nanotube. Angewandte Chemie International Edition. 2019 Jan 14;58(3):844-8

17. Chen, C., Ni, X., Tian, H.W., Liu, Q., Guo, D.S., Ding, D.: Calixarene-Based Supramolecular AIE Dots with Highly Inhibited Nonradiative Decay and Intersystem Crossing for Ultrasensitive Fluorescence Image-Guided Cancer Surgery.Angewandte Chemie International Edition. 2020 Jun15;59(25):10008−12

18. Jiao, F., Wu, X., Jian, T., Zhang, S., Jin, H., He, P., Chen, C.L., De Yoreo, J.J.: Hierarchical Assembly of Peptoid-Based Cylindrical Micelles Exhibiting Efficient Resonance Energy Transfer in Aqueous Solution. Angew. Chem. **26**(35), 12351−12358 (2019 Aug)

19. Schwarz, K.: DFT calculations of solids with LAPW and WIEN2k.Journal of Solid State Chemistry. 2003 Dec1;176(2):319−28

20. Blaha, P., Schwarz, K., Madsen, G.K., Kvasnicka, D., Luitz, J.: wien2k. An augmented plane wave + local orbitals program for calculating crystal properties. (2001)

21. Naito, T., Roca-Maza, X., Colò, G., Liang, H.: Coulomb exchange functional with generalized gradient approximation for self-consistent Skyrme Hartree-Fock calculations. Phys. Rev. C. **13**(2), 024309 (2019 Feb)

22. Wu, Z., Cohen, R.E.: More accurate generalized gradient approximation for solids.Physical Review B. 2006 Jun20;73(23):235116

23. Rahnamaye, A.H.: Effects of IIIB transition metals on optoelectronic and magnetic properties of HoMnO3: A first principles study. Chin. Phys. B. **9**(11), 117102 (2015 Oct)

24. Nyayban, A., Panda, S., Chowdhury, A., Sharma, B.I.: First principle studies on the optoelectronic properties of rubidium lead halides. arXiv preprint arXiv:1909.11419. Sep25. (2019)

25. Salehi, H., Tolabinejad, H.: First-principles study of the optical properties of SrHfO3. Optics and Photonics Journal. Jun 28;1(2):75–80. (2011)

26. Olmon, R.L., Slovick, B., Johnson, T.W., Shelton, D., Oh, S.H., Boreman, G.D., Raschke, M.B.: Optical dielectric function of gold.Physical Review B. 2012 Dec28;86(23):235147

27. Liberal, I., Engheta, N.: Near-zero refractive index photonics. Nat. Photonics. **11**(3), 149 (2017 Mar)

28. Li, J., Wu, S.T.: Extended Cauchy equations for the refractive indices of liquid crystals. Journal of applied physics. 2004 Feb 1;95(3):896–901

29. Egerton, R.F.: Electron energy-loss spectroscopy in the TEM.Reports on Progress in Physics. 2008 Dec16;72(1):016502

30. Aliabad, H.R., Rabbanifar, S., Khalid, M.: Structural, optoelectronic and thermoelectric properties of FeSb2 under pressure: Bulk and monolayer. Phys. B: Condens. Matter. **1**, 570:100–109 (2019 Oct)
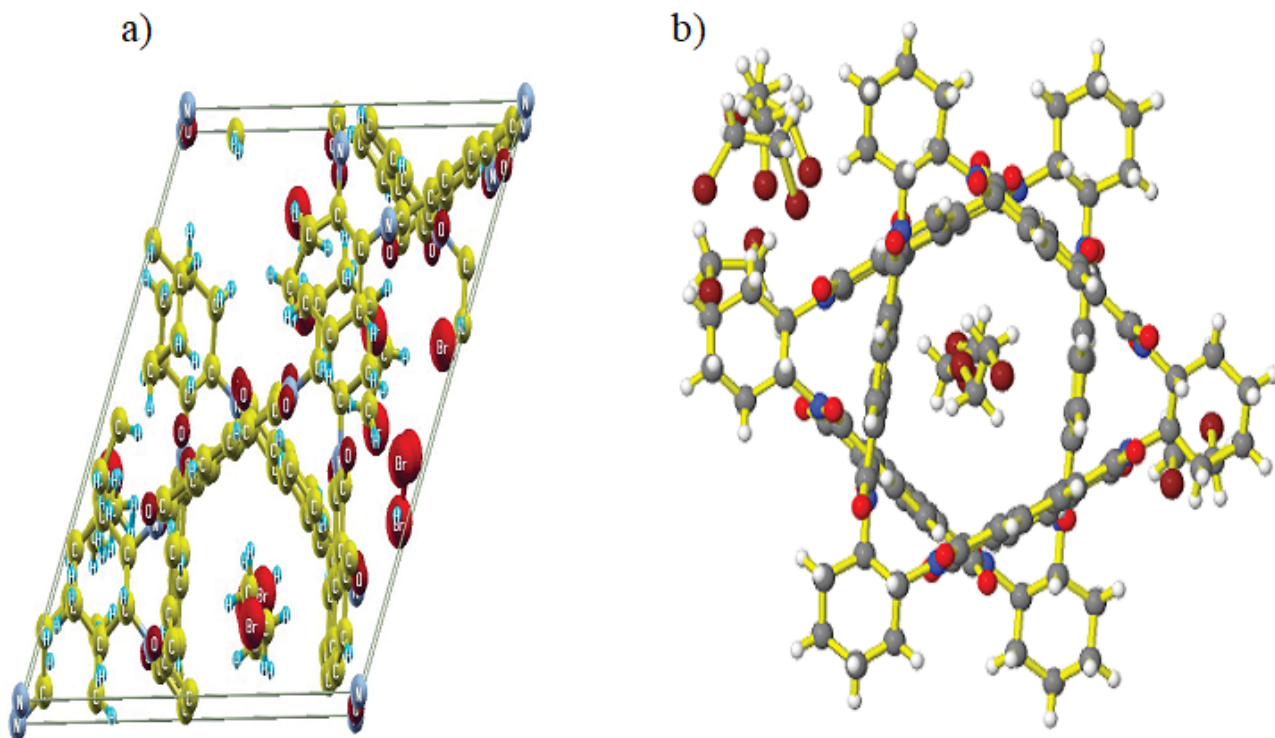
Figures

a)

b)

Figure 1

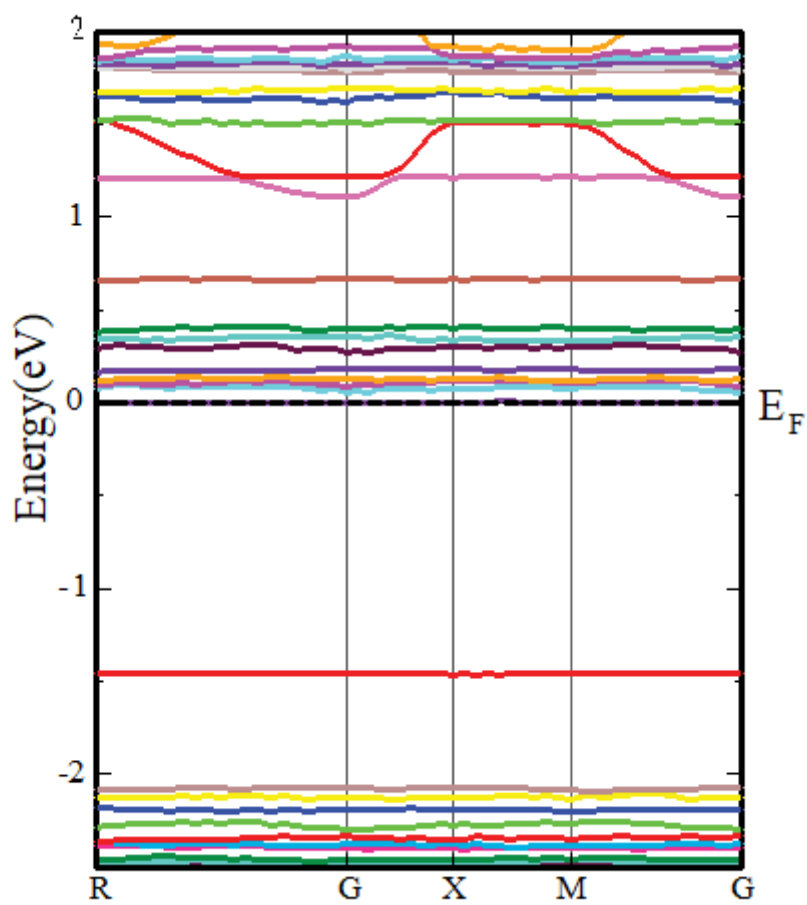Crystal structure of $C_{66}H_{54}Br_6N_6O_{12}$ compound

Figure 2

Calculated band structures for $C_{66}H_{54}Br_6N_6O_{12}$ by GGA
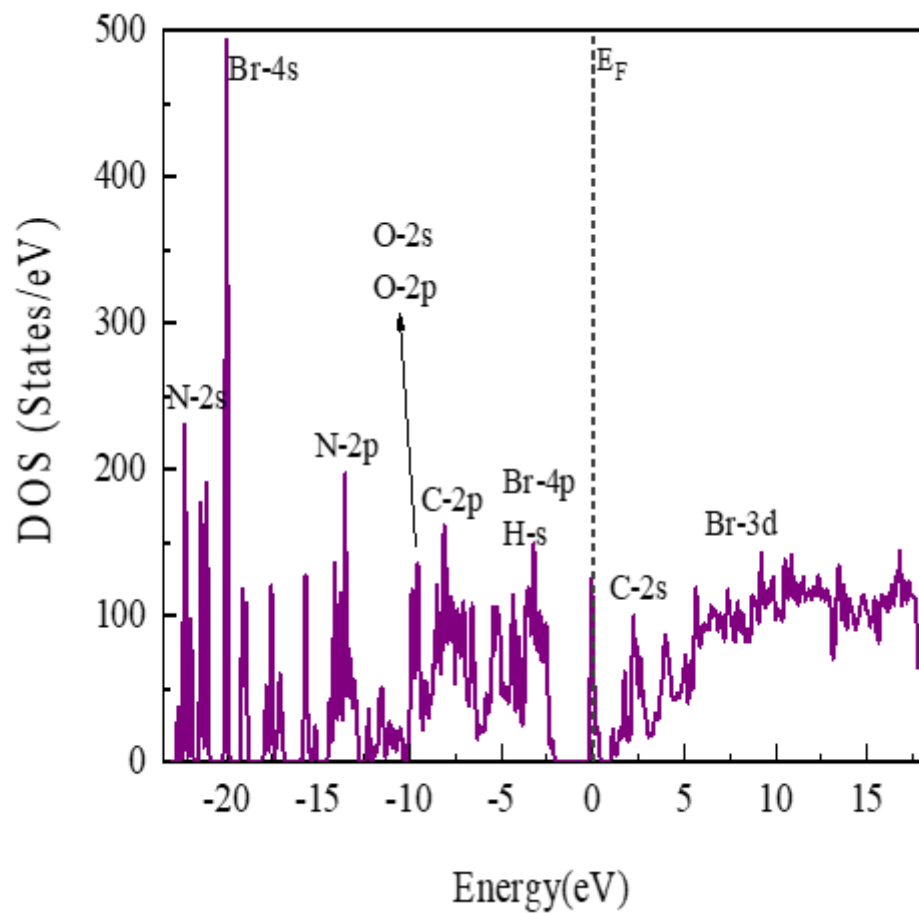
Figure 3

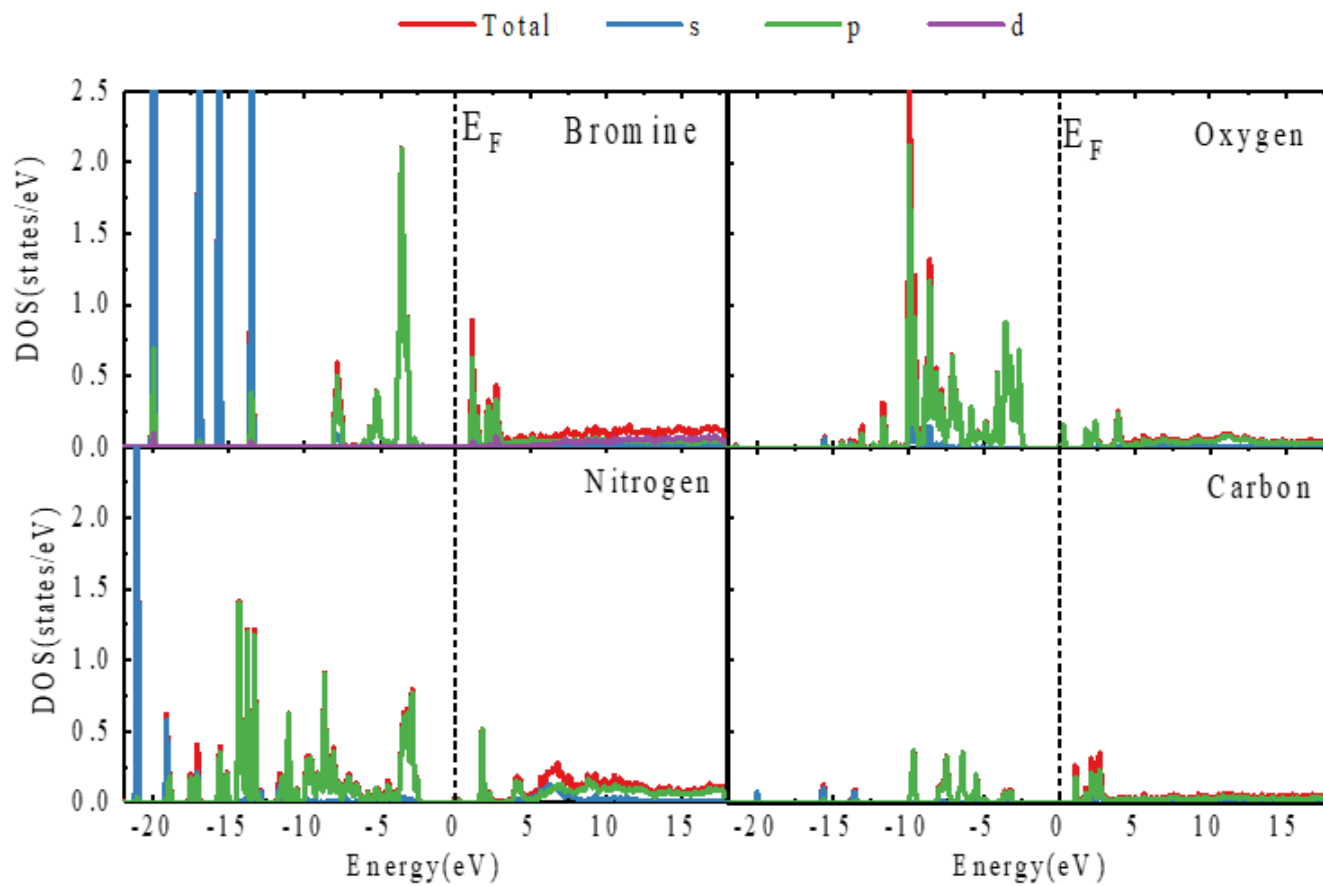Calculated total of DOS for $C_{66}H_{54}Br_6N_6O_{12}$ by GGA

Figure 4

Calculated DOS for $C_{66}H_{54}Br_6N_6O_{12}$ by GGA for **a)** carbon orbitals, **b)** Hydrogen orbital, **c)** Beryllium orbitals, **d)** Nitrogen orbitals, **e)** Oxygen orbitals
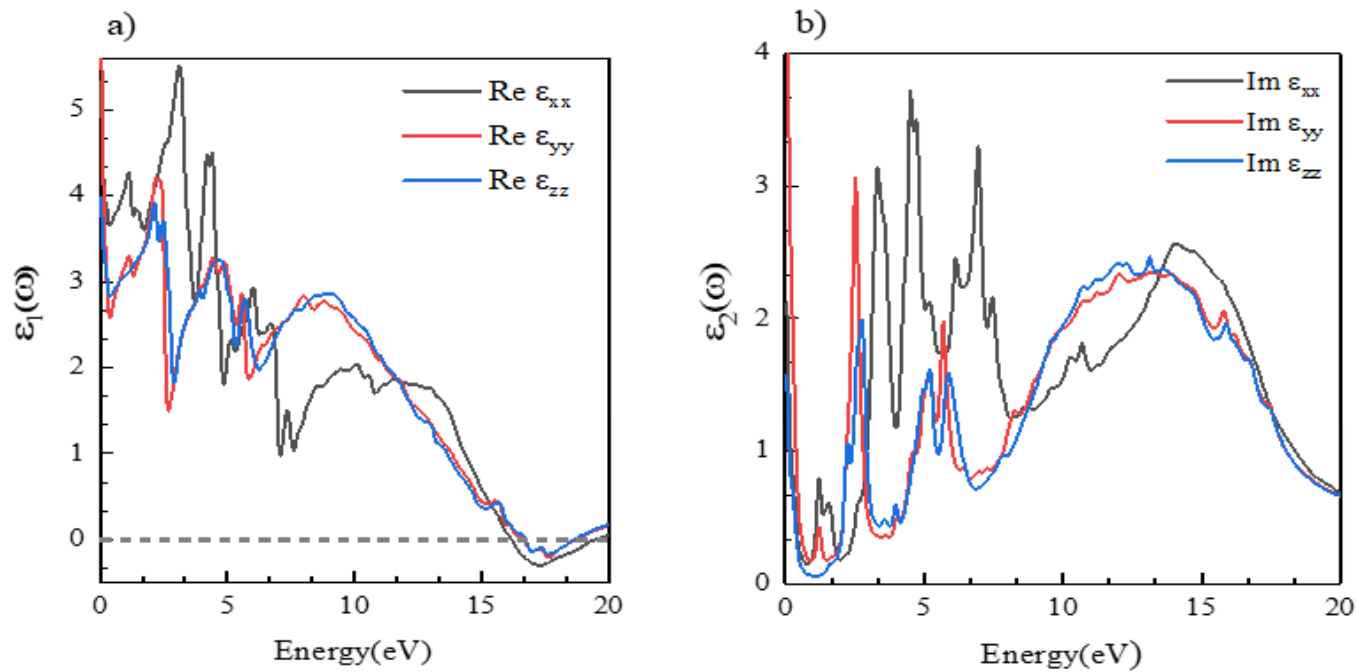
Figure 5

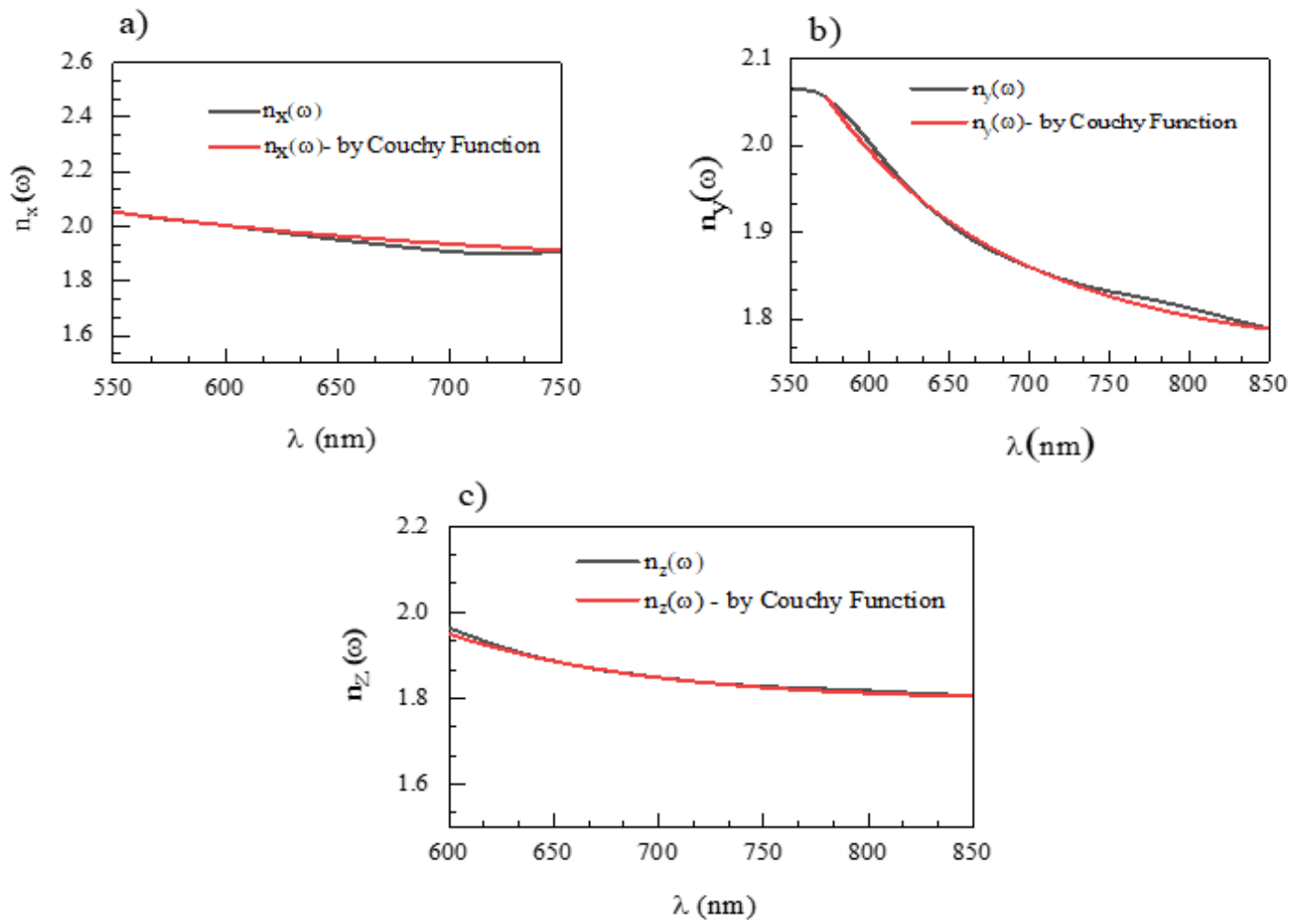Dielectric functions of $C_{66}H_{54}Br_6N_6O_{12}$ compound **(a)** real part **(b)** imaginary part

Figure 6

Refractive index of $C_{66}H_{54}Br_6N_6O_{12}$ compound and conformity of Cauchy's equation with it in **(a)** x direction **(b)** y direction **(c)** z direction
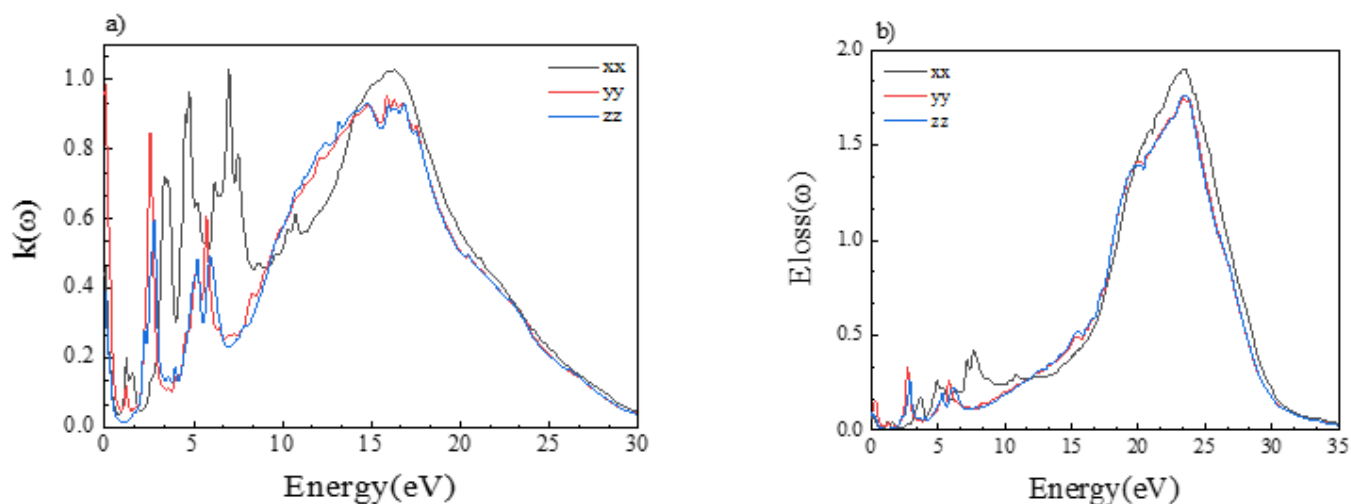
Figure 7

a) Extinction coefficient of $C_{66}H_{54}Br_6N_6O_{12}$ compound in three dimensions b) Calculated EELS of $C_{66}H_{54}Br_6N_6O_{12}$ compound in three dimensions
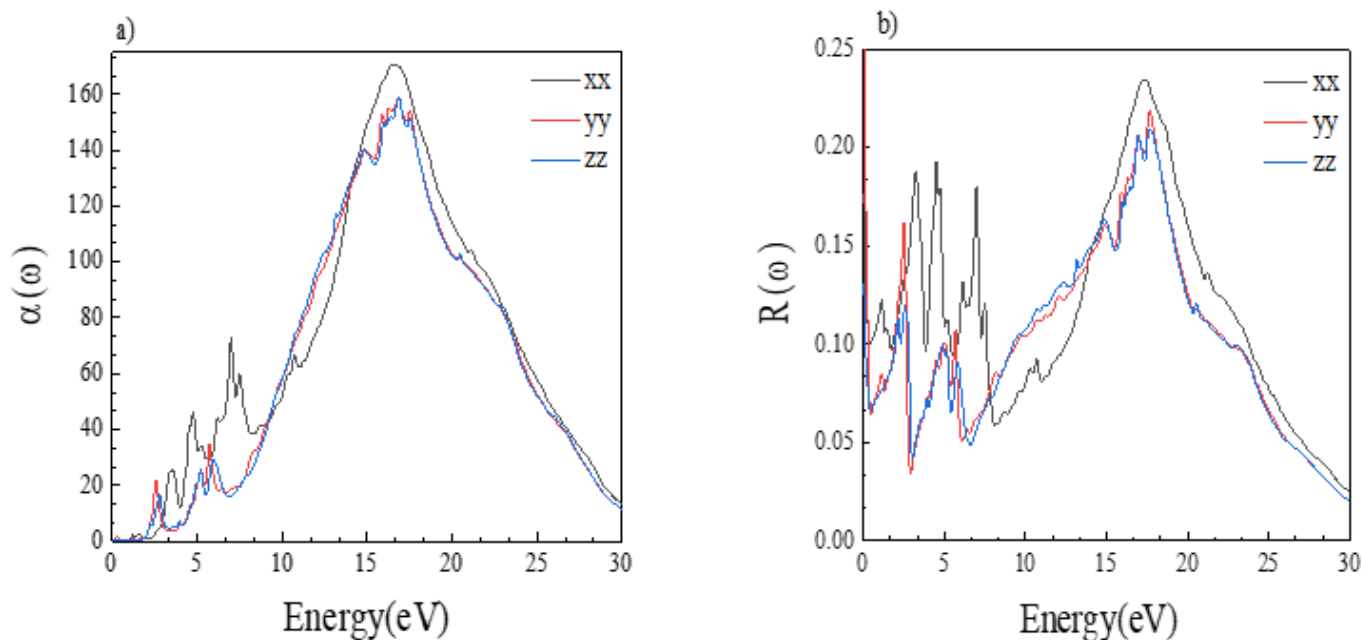

Figure 8

a) Absorption coefficient of $C_{66}H_{54}Br_6N_6O_{12}$ compound in three dimensions b) Reflection coefficient of $C_{66}H_{54}Br_6N_6O_{12}$ compound in three dimensions